Mathematical Biosciences and Engineering

MBE, 20(2): 4018–4039.
DOI: 10.3934/mbe.2023188
Received: 13 October 2022
Revised: 26 November 2022
Accepted: 08 December 2022
Published: 16 December 2022

http://www.aimspress.com/journal/MBE

Research article

Identification of an endoplasmic reticulum stress-related gene signature to predict prognosis and potential drugs of uterine corpus endometrial cancer

Pei Zhou[1,†], Caiyun Wu[2,†], Cong Ma[2], Ting Luo[2], Jing Yuan[1], Ping Zhou[2,*] and Zhaolian Wei[2,*]

[1] Prenatal Diagnosis Center, Department of Obstetrics and Gynecology, First Affiliated Hospital of Anhui Medical University, Hefei 230022, China
[2] Reproductive Medicine Center, Department of Obstetrics and Gynecology, First Affiliated Hospital of Anhui Medical University, Hefei 230022, China

† The authors contributed equally to this work.

* **Correspondence:** Email: weizhaolian_1@126.com, Tel: 055165908446; zhoup325@126.com, Tel: 055165908421.

Abstract: Uterine corpus endometrial cancer (UCEC) is the sixth most common female cancer worldwide, with an increasing incidence. Improving the prognosis of patients living with UCEC is a top priority. Endoplasmic reticulum (ER) stress has been reported to be involved in tumor malignant behaviors and therapy resistance, but its prognostic value in UCEC has been rarely investigated. The present study aimed to construct an ER stress-related gene signature for risk stratification and prognosis prediction in UCEC. The clinical and RNA sequencing data of 523 UCEC patients were extracted from TCGA database and were randomly assigned into a test group (n = 260) and training group (n = 263). An ER stress-related gene signature was established by LASSO and multivariate Cox regression in the training group and validated by Kaplan-Meier survival analysis, Receiver Operating Characteristic (ROC) curves and nomograms in the test group. Tumor immune microenvironment was analyzed by CIBERSORT algorithm and single-sample gene set enrichment analysis. R packages and the Connectivity Map database were used to screen the sensitive drugs. Four ERGs (ATP2C2, CIRBP, CRELD2 and DRD2) were selected to build the risk model. The high-risk group had significantly reduced overall survival (OS) ($P < 0.05$). The risk model had better prognostic accuracy than clinical factors. Tumor-infiltrating immune cells analysis depicted that CD8+ T cells and regulatory T cells

were more abundant in the low-risk group, which may be related to better OS, while activated dendritic cells were active in the high-risk group and associated with unfavorable OS. Several kinds of drugs sensitive to the high-risk group were screened out. The present study constructed an ER stress-related gene signature, which has the potential to predict the prognosis of UCEC patients and have implications for UCEC treatment.

Keywords: uterine corpus endometrial cancer; endoplasmic reticulum stress; gene signature; prognosis; immunotherapy

1. Introduction

According to a global cancer report, uterine corpus cancer ranks as the sixth most common cancer in women, with approximately 417,000 new cases (2.2% of all sites) and 97,000 deaths (1.0% of all sites) in 2020 worldwide [1]. Among all American female cancer survivors, uterine corpus cancer is the second most prevalent after breast cancer [2]. More than 90% of uterine corpus cancer originated from the endometrium, namely, uterine corpus endometrial cancer (UCEC) [2]. Due to early detection and improved treatment, the 5-year overall survival rate of uterine corpus cancer is about 81% [2], but the mortality rate of UCEC remains the highest among women with low socioeconomic status [3]. Considering the growing morbidity and large number of surviving UCEC patients, it is imperative to explore biomarkers to predict prognosis and guide treatment.

The endoplasmic reticulum (ER) is an organelle involved in multiple cellular processes, including protein synthesis, folding and transport, lipid biosynthesis and calcium balance [4]. However, in the tumor microenvironment, many harsh factors can disrupt the protein-handling capacity of ER and cause excessive accumulation of misfolded/unfolded protein, such as nutrient starvation, oxidative stress, intracellular calcium imbalance and high metabolic demand, thereby leading to a state of "ER stress" [5]. Subsequently, unfolded protein response (UPR) is activated in an attempt to restore ER homeostasis, ultimately causing cellular reprogramming and adaptation, autophagy or even cell death [6]. A body of studies has indicated that sustained and robust ER stress responses contribute to cancer cell survival, metastasis, angiogenesis and therapy resistance [7–9]. In addition, ER stress responses can play an immunoregulatory role [10]. ER stress-related genes (ERGs), a series of genes involved in the ER stress signaling, have been reported to correlate with various tumors' development, such as breast, glioma, liver and prostate cancer [11–14]. However, the roles and therapeutic value of ERGs in UCEC have not been extensively investigated. It was reported that the UPR target glucose-regulated protein 78 took part in the endometrial cancer cell growth, invasion and chemotherapy resistance and was correlated with advanced stage and poor prognosis [15,16]. Therefore, ERGs may be valuable prognostic factors and potential therapeutic avenues for UCEC.

As a patient's prognosis exerts a great influence on personal and clinical decisions, accurate prognostic models have gained great attention in recent years [17,18]. The present study aimed to construct a risk model based on ERGs to forecast clinical outcomes and provide guidance for UCEC treatment. By bioinformatic analysis, we constructed a prognostic gene signature containing 4 ERGs, which exhibited excellent prognostic capacity. In addition, based on the model, we analyzed the immune infiltration and drug sensitivity in order to improve the prognosis of UCEC patients.

2. Materials and methods

2.1. Data preparation

RNA sequencing of transcriptome profiling data (HTSeq-FPKM) and corresponding clinical information for UCEC were obtained from TCGA database (https://portal.gdc.cancer.gov/repository), containing 554 malignancy samples and 32 normal samples. We obtained the clinical data of 548 UCEC cases, including survival time, survival status, age, gender, grade and stage. After eliminating the samples with survival time < 30 days and unknown survival time or status, 523 UCEC patients were ultimately retained in our study. What's more, 1371 ERGs were extracted from GeneCards (https://www.genecards.org/) with relevance score > 5. The "limma" R package and Wilcoxon test were used to identify differentially expressed ERGs (DEERGs) between UCEC tumor and normal samples, with the significance thresholds set as $|\text{Log}_2 \text{ fold change (FC)}| > 1$ and false discovery rate (FDR) < 0.05 [19]. Finally, 351 DEERGs were obtained for further analysis (Table S1). To identify the potential biological functions of hub DEERGs, we did Gene Ontology (GO) term and Kyoto Encyclopedia of Genes and Genomes (KEGG) pathway enrichment analysis by "GOplot," "enrichplot" and "ggplot2" R packages (https://bioconductor.org/packages/release/bioc/html/enrichplot.html) [20, 21]. GO terms contain biological process (BP), cellular components (CC) and molecular functions (MF) analysis. The results were visualized with "clusterProfiler" and "org.Hs.eg.db" R packages (https://www.bioconductor.org/packages/release/data/annotation/html/org.Hs.eg.db.html) [22].

2.2. Risk model construction

351 DEERGs' transcriptome data and 523 UCEC clinical data were integrated by the "limma" R package, and they were then randomly assigned into test and training groups, with 260 and 263 samples, respectively. The training group was used to establish the risk signature, while the test group and entire group were used to verify its effectiveness. First, by univariate Cox regression, we obtained 7 candidate prognostic ERGs in the training group with the significant P value < 0.001. Next, these ERGs were subjected to least absolute shrinkage and selection operator (LASSO) regression to exclude overfitting genes and select more robust biomarkers [23,24]. As a result, 4 ERGs were selected and identified as the prognostic biomarkers of UCEC ($P < 0.05$). Finally, multivariate Cox regression was performed to establish a risk score system. The risk score was calculated as follows: risk score = $\sum_{i=1}^{n} \text{Coef}_i \times \text{Exp}_i$, where the Coef represents the coefficient calculated by multivariate Cox regression, and the Exp represents the expression level of 4 hub ERGs.

2.3. Survival analysis

The test group was further classified into high risk and low risk subgroups based on the median risk score of the training group. There were totally 256 samples of the high-risk group and 267 samples of the low-risk group in our study. Overall survival (OS) of UCEC patients between the high and low risk groups was compared by Kaplan-Meier survival analysis and log-rank test using "survival" and "survminer" R packages (https://CRAN.R-project.org/package = survival, https://rpkgs.datanovia.com/survminer/index.html). In addition to OS analysis, we grouped all patients

according to their clinical characteristics (age ≤ 60 or > 60, grade I-II or III, stage I-II or III-IV) and compared their survival between high and low risk groups, respectively. We also analyzed the association of the 4 hub ERGs with OS.

2.4. Prognostic accuracy validation of the risk model

Receiver Operating Characteristic (ROC) curves were plotted to indicate the value of the constructed risk model in predicting survival at 1, 3 and 5 years using "timeROC" R package [25]. The predictive efficacy of the risk model and clinical variables (age, grade and stage) was compared using the area under the ROC curve (AUC). To determine whether the risk signature was an independent prognostic predictor, we employed univariate and multivariate regression analyses with the risk score and clinical factors. Principal component analysis (PCA) and t-distributed stochastic neighbor embedding (t-SNE), linear and non-linear dimensionality reduction methods, respectively, were performed by "Rtsne" (https://github.com/jkrijthe/Rtsne) and "ggplot2" R packages to detect the transcriptomic heterogeneity, thereby further confirming the feasibility of the risk model [21,26].

2.5. Nomogram and calibration

Nomograms are popular prognostic tools which can integrate multiple clinical and biological prognostic factors to generate an individualized probability of a certain clinical event [27]. Nomograms based on the risk, age, grade and stage were developed to predict the 1-, 3- and 5-year survival probabilities of UCEC patients using "survival," "rms" and "regplot" R packages (https://hbiostat.org/R/rms, https://cran.r-project.org/web/packages/regplot/index.html). The calibration plot demonstrated the consistency between the nomogram predicted OS and observed OS at 1, 3 and 5 years. The concordance index (C-index) curve was plotted to estimate the predictive consistence among risk score, grade and stage using "dplyr," "survival," "rms" and "pec" R packages (https://dplyr.tidyverse.org) [28].

2.6. Gene set enrichment analysis

Gene Set Enrichment Analysis (GSEA) Version 4.2.1 is freely available software that analyzes genes with common biological characteristics, such as function, chromosomal location or regulation [29]. By estimating enrichment score (ES), assessing significance, adjusting for multiple hypothesis testing and ultimately calculating an FDR q value, it can identify the distribution of gene sets in phenotypic distinction on the gene expression level. We conducted GESA to distinguish significantly enriched KEGG and GO pathways between high and low risk groups. If the ES > 0, the functional pathway was significantly enriched in the high-risk group; otherwise, it was active in the low-risk group. We took the top 10 KEGG pathways with the largest absolute value of normalized enrichment score (NES) and plotted a multi GSEA enrichment map via the "plyr," "ggplot2," "grid" and "gridExtra" R packages (https://github.com/pmur002/gridgraphics) [30].

2.7 Tumor immune microenvironment analysis

To analyze the tumor microenvironment of all UCEC samples, we calculated the stromal score, immune score and ESTIMATE score to evaluate the tumor purity using the "estimate" R package [31].

The higher the tumor microenvironment score is, the lower the tumor purity. In addition, we visualized and compared 22 tumor-infiltrating immune cells (TIICs) between high and low risk groups among all UCEC samples via the CIBERSORT algorithm [32]. By "limma," "survival" and "survminer" R packages, we merged survival data and CIBERSORT results of all UCEC patients, and we then compared the survival probability of different TIICs between high and low risk groups. Survival curves were plotted for TIICs with $P < 0.05$. To further indicate the differences of immune status between high and low risk groups, single-sample gene set enrichment analysis (ssGSEA) was performed to compare the infiltrating scores of 13 immune functions and 16 immune cells via the "GSVA," "limma" and "GSEABase" R packages (https://bioconductor.org/packages/GSEABase/) [19,33].

2.8 Drug sensitivity analysis

The R package "pRRophetic" was used to predict the drug sensitivity by estimating the half-maximal inhibitory concentration (IC50), thereby filtering out potential anti-UCEC drugs [34]. The drug sensitivity differences were compared between high and low risk groups with the significance *P* value < 0.001. The correlations between the risk score and drug sensitivity were evaluated by Spearman's correlation analysis. Connectivity Map (CMap) (https://clue.io) is a database which collects gene expression profiles of human cells exposed to various small molecules. It connects genes, drugs and diseases by comparing drug-specific gene expression profiles with a disease-specific gene signature via nonparametric rank-based Kolmogorov-Smirnov test [35]. We uploaded the query files of the differentially expressed genes between high and low risk groups in an effort to identify candidate drugs for UCEC.

2.9 Statistical analysis

Strawberry Perl (Version 5.32.1 for Windows 64-bit) was used to prepare the data. All statistical analyses were performed using R software (version 4.2.1 for Windows 64-bit). The "limma" R package and Wilcoxon test were used to identify differently expressed genes between tumor and normal tissues. Wilcoxon test was also employed to compare 22 TIICs' proportions between two risk groups. Spearman's correlation analysis was applied to evaluate the association between risk score and drug sensitivity. $P < 0.05$ was considered statistically significant unless otherwise specified.

3. Results

3.1. Identification of differently expressed ERGs

The flow diagram is exhibited in Figure 1. 351 DEERGs were identified among 554 UCEC samples and 35 normal samples with $|\text{Log}_2\text{ FC}| > 1$ and FDR < 0.05. Of them, 202 were upregulated with $\log_2\text{FC} > 1$, and 149 were downregulated with $\log_2\text{FC} < -1$ (Figure 2A). The expression of the top 50 DEERGs is shown in the heat map (Figure 2B). The GO term enrichment analysis showed that the 351 DEERGs mainly took part in the biological processes of cellular divalent inorganic cation homeostasis, calcium ion homeostasis and transport and divalent metal ion transport, whose cellular component was mainly endoplasmic reticulum lumen, and the molecular functions were mainly passive transmembrane transporter activity and channel activity (Figure 2C). KEGG pathway analysis showed these DEERGs were significantly associated with the pathways of neurodegeneration and

multiple disease (Figure 2D).

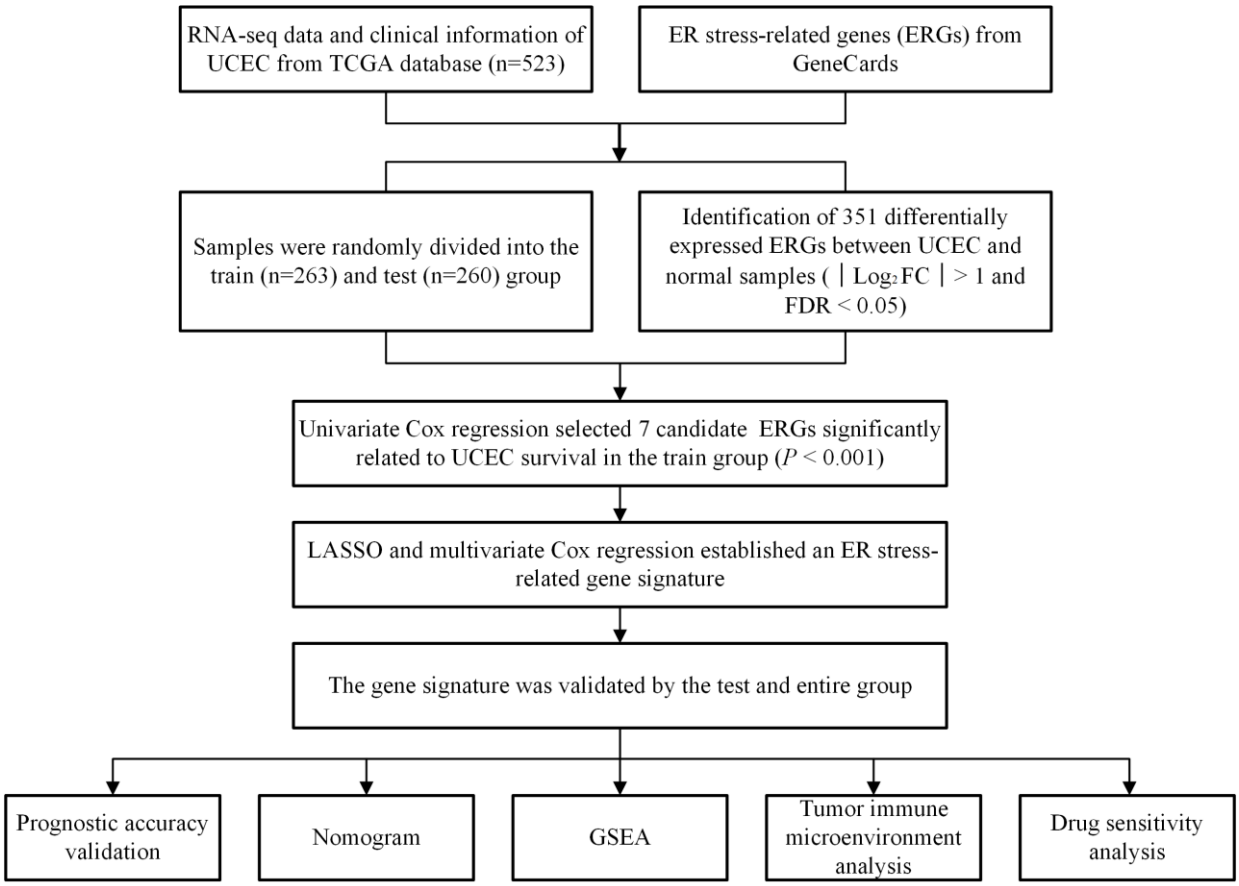

Figure 1. Flowchart of the study. UCEC: Uterine corpus endometrial cancer, FC: fold change, FDR: false discovery rate, LASSO: least absolute shrinkage and selection operator, GSEA: gene set enrichment analysis.

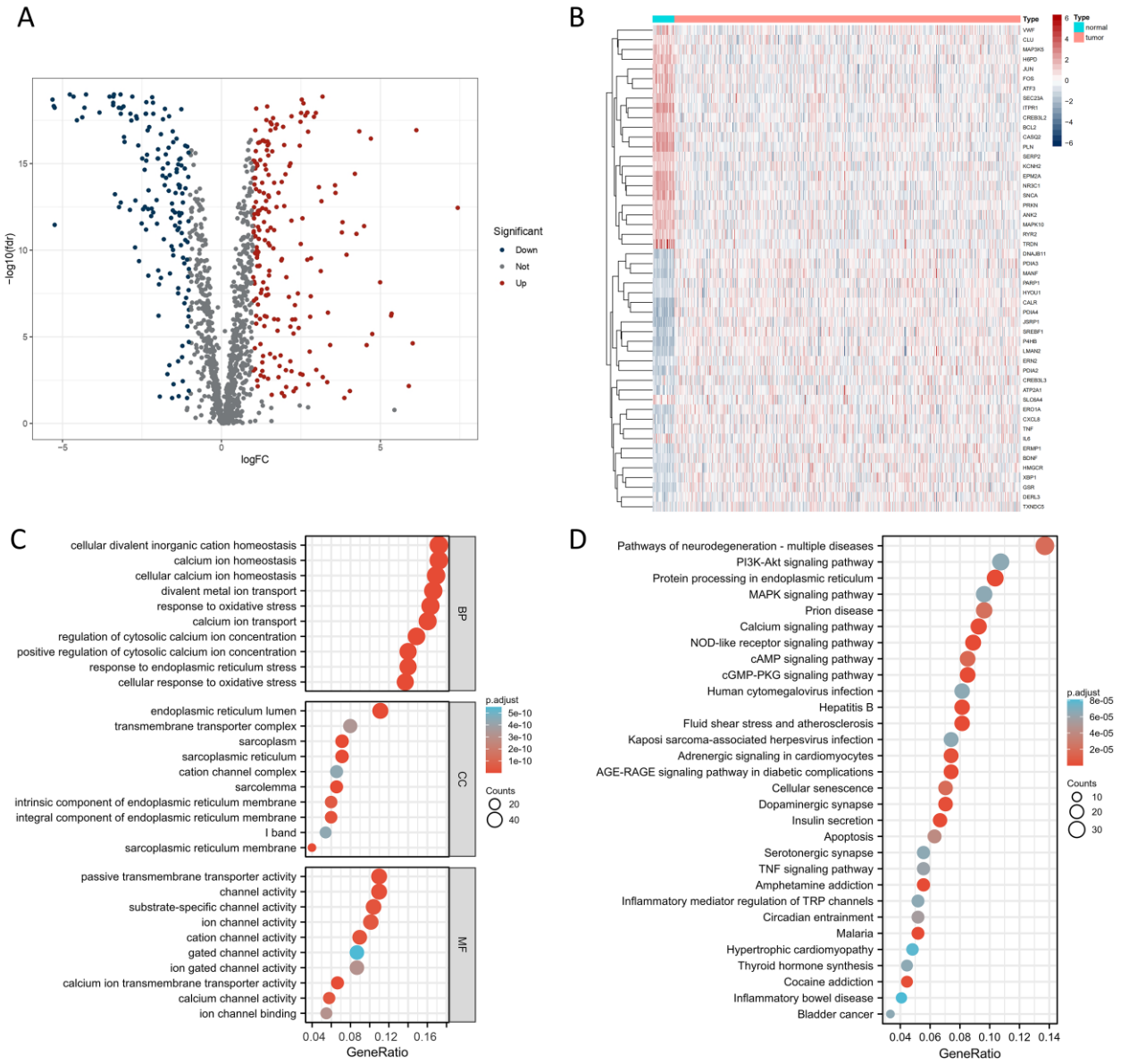

Figure 2. Identification of differently expressed endoplasmic reticulum stress related genes (DEERGs) between UCEC and normal samples. (A) Volcano plot of DEERGs. 202 were upregulated and 149 were downregulated in UCEC samples compared with normal samples. (B) The heatmap of the top 50 DEERGs. (C) GO term enrichment analysis of DEERGs in biological process (GO-BP), cellular component (GO-CC) and molecular function (GO-MF). (D) KEGG pathway analysis of DEERGs.

3.2. Construction of ER stress-related gene signature in UCEC

The 351 DEERGs were subjected to univariate Cox regression analysis in the training group, and 7 of them were shown to be significantly associated with OS of UCEC patients with $P < 0.001$ (Figure 3A). Then, the 7 genes were introduced into LASSO Cox regression analysis to identify the most predictive gene. Consequently, 4 genes were obtained to build the prognostic model: namely, ATPase secretory pathway Ca2+ transporting 2 (ATP2C2), cold inducible RNA binding protein

(CIRBP), cysteine rich with EGF like domains 2 (CRELD2) and dopamine receptor D2 (DRD2) (Figure 3B,C). Multivariate Cox regression analysis of the 4 genes was performed to create the risk signature (Table 1). Ultimately, the risk score = (0.7845*expression value of DRD2) + (-0.6562*expression value of CIRBP) + (-0.4710 *expression value of CRELD2) + (-0.4241*expression value of ATP2C2). Among the 4 genes, DRD2 was a risk factor for UCEC patients' prognosis with hazard ratio (HR) > 1, while the remaining 3 genes were protective factors. We further explored the association between the expression levels of the 4 genes with survival in all UCEC cases. The survival curves illustrated that high expression of DRD2 was correlated with poor OS, but high expression of CIRBP, CRELD2 and ATP2C2 contributed to favorable OS (Figure 3D–G), which was consistent with the multivariate Cox regression analysis.

Table 1. Multivariate Cox regression analysis of the 4 hub genes in the training group of UCEC.

ID	Coefficient	HR	HR.95L	HR.95H	*P* value
DRD2	0.7845	2.1912	1.2044	3.9864	0.0102
CIRBP	-0.6562	0.5188	0.3163	0.8512	0.0094
CRELD2	-0.4710	0.6244	0.4004	0.9736	0.0377
ATP2C2	-0.4241	0.6544	0.4418	0.9691	0.0343

HR: hazard ratio, HR.95L: lower 95% confidence interval of HR, HR.95H: higher 95% confidence interval of HR.

Table 2. Gene set enrichment analysis of differentially expressed genes between high and low risk groups in gene ontology.

Group	Name	Size	ES	NES	FDR
High-risk group	GOBP-nerve development	81	0.588	2.232	0.099
	GOBP-positive regulation of synapse assembly	62	0.652	2.202	0.077
	GOMF-voltage gated sodium channel activity	25	0.715	2.147	0.047
	GOMF-GABA receptor activity	22	0.733	2.111	0.032
	GOCC-voltage gated channel complex	17	0.791	2.188	0.047
	GOCC-presynaptic membrane	142	0.541	2.097	0.034
Low-risk group	GOBP-cilium movement	179	-0.711	-2.308	0.002
	GOBP-sperm motility	119	-0.645	-2.259	0.005
	GOMF-oxidoreductase activity acting on a sulfur group of donors	58	-0.617	-2.129	0.016
	GOMF-nucleoside diphosphate kinase activity	18	-0.759	-2.088	0.022
	GOCC-motile cilium	223	-0.678	-2.339	0.003
	GOCC-9plus2 motile cilium	146	-0.658	-2.310	0.003

GO: gene ontology, BP: biological process, MF: molecular function, CC: cellular component, Size: the number of genes enriched, ES: enrichment score, NES: normalized enrichment score, FDR: false discovery rate.

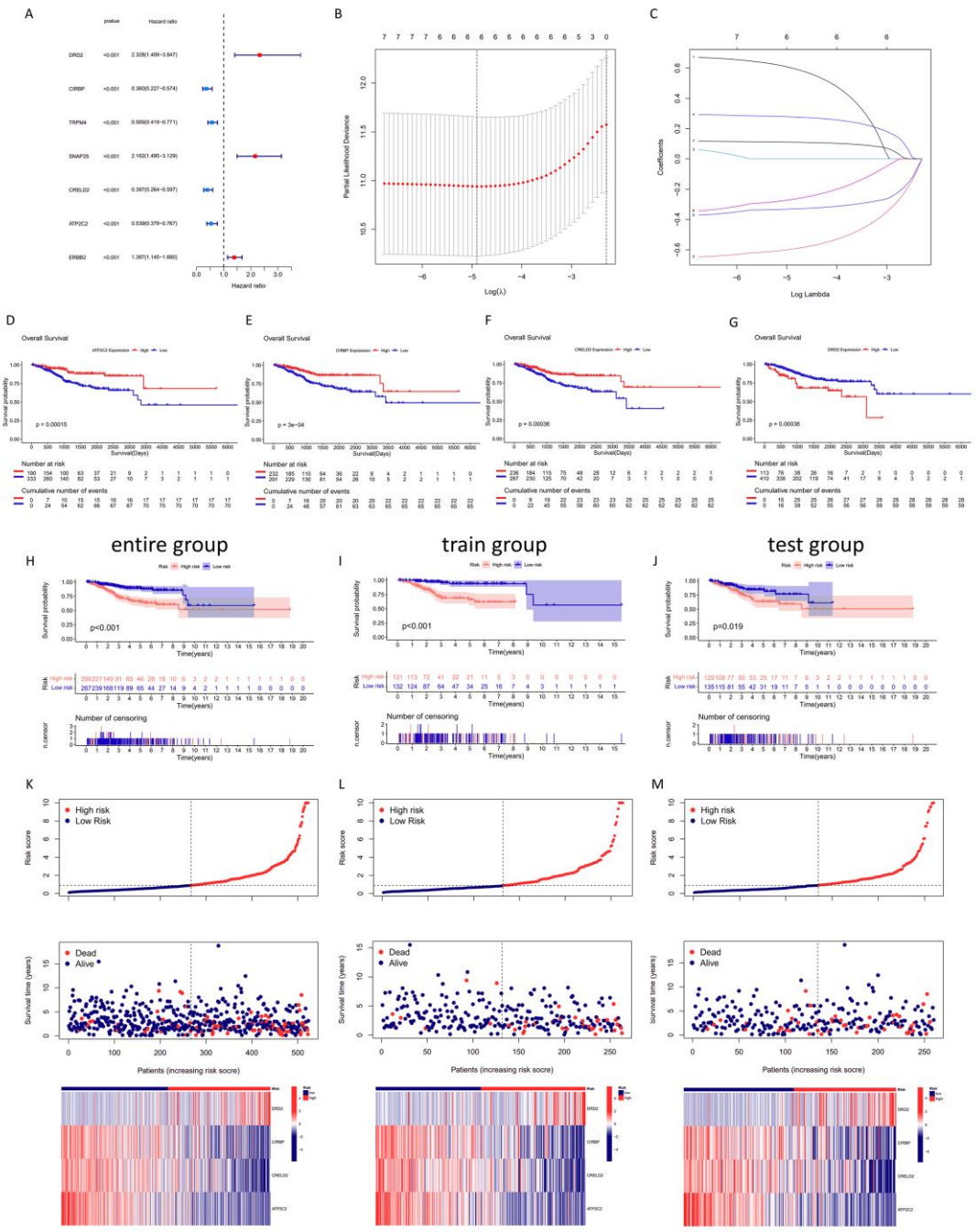

Figure 3. Construction and validation of an ER stress-related gene signature in UCEC. (A) Univariate Cox regression analysis of differentially expressed ERGs (DEERGs) in the training group (n = 263) to identify survival related ERGs. (B) Cross-validation to determine the number of parameters in the LASSO regression model. (C) The LASSO coefficient profiles of 7 survival related DEERGs. (D–G) The correlation between expression levels of 4 hub genes with overall survival of UCEC patients by Kaplan-Meier survival analysis and log rank test. (H–J) Kaplan-Meier survival curves of different risk groups in entire group, train group and test group, respectively. (K–M) Layout of risk scores, survival status of each UCEC patient and expression heatmap of 4 hub ERGs in entire group, training group and test group, respectively. In the training group, in the high-risk group, n = 131; in the low-risk group, n = 132. In the test group, in the high-risk group, n = 125; in the low-risk group, n = 135.

3.3. Verification of the four ERGs' prognostic signature in UCEC

All the UCEC cases were classified into high and low risk groups according to the median risk score of the training group; thereby, there were 131 and 132 cases of high and low risk, respectively, in the training group and 125 and 135 cases of high and low risk, respectively, in the test group. The high-risk group showed reduced OS whether in the entire, test or training group (Figure 3H–J). The risk score distribution, survival status of each UCEC patient and expression heatmap of 4 hub genes in the entire, test and training groups are also shown in Figure 3K–M respectively. The expression heatmap displayed the upregulation of DRD2 and the downregulation of ATP2C2, CIRBP and CRELD2 in the high-risk group in both the test and training sets, which totally coincided with the above mentioning that DRD2 may be a risk factor.

We performed a univariate Cox regression algorithm on the entire group to identify potential prognostic factors, including age, grade, stage and risk score. As shown in Figure 4A, they were all potential risk factors for unfavorable clinical outcome of UCEC ($P < 0.05$). To explore the prognostic independence of risk score, we applied multivariate Cox regression analysis. It turned out that risk signature was still an independent survival predictor ($P < 0.05$, HR > 1) (Figure 4B). We further classified UCEC patients according to their clinical characteristics to evaluate the prognostic value of the risk signature. Patients with low risk score showed better OS (all $P < 0.05$), and the trends exhibited high consistence between patients with age ≤ 60 and > 60, grade I-II and III and stage I-II and III-IV (Figure 4C–E), which reflected the solid prognostic feasibility of the risk score.

Time dependent ROC curves further elucidated that the AUC values of risk score for predicting 1, 3, and 5-year survival in the training group were 0.807, 0.793 and 0.769, respectively; and those in the test group were 0.695, 0.652 and 0.664, respectively, indicating that the ER stress related risk model processed moderate prognostic accuracy in UCEC (Figure 4F–H). Compared with age, grade and stage, the AUC of risk score was the highest and reached 0.736, showing the better prognostic sensitivity and specificity of risk score compared to these clinical factors (Figure 4I). Also, the C-indexes among risk score, grade and stage were satisfactory, about 0.7, which also reflected the accuracy of the risk model (Figure 4J). To predict the 1, 3, and 5-year survival probability of each specific UCEC patient, we constructed a nomogram with clinical variables and risk score (Figure 4K). The higher the total points were, the poorer the prognosis. The calibration curve showed the nomogram predicted 1,3,5-year OS highly matched the observed OS (Figure 4L). PCA and t-SNE plots indicated that the gene expression patterns between high and low risk groups were clearly separated after dimensionality reduction (Supplementary Figure 1). All of the above confirmed that the ERG-related risk model was a powerful and reliable outcome predictor of UCEC.

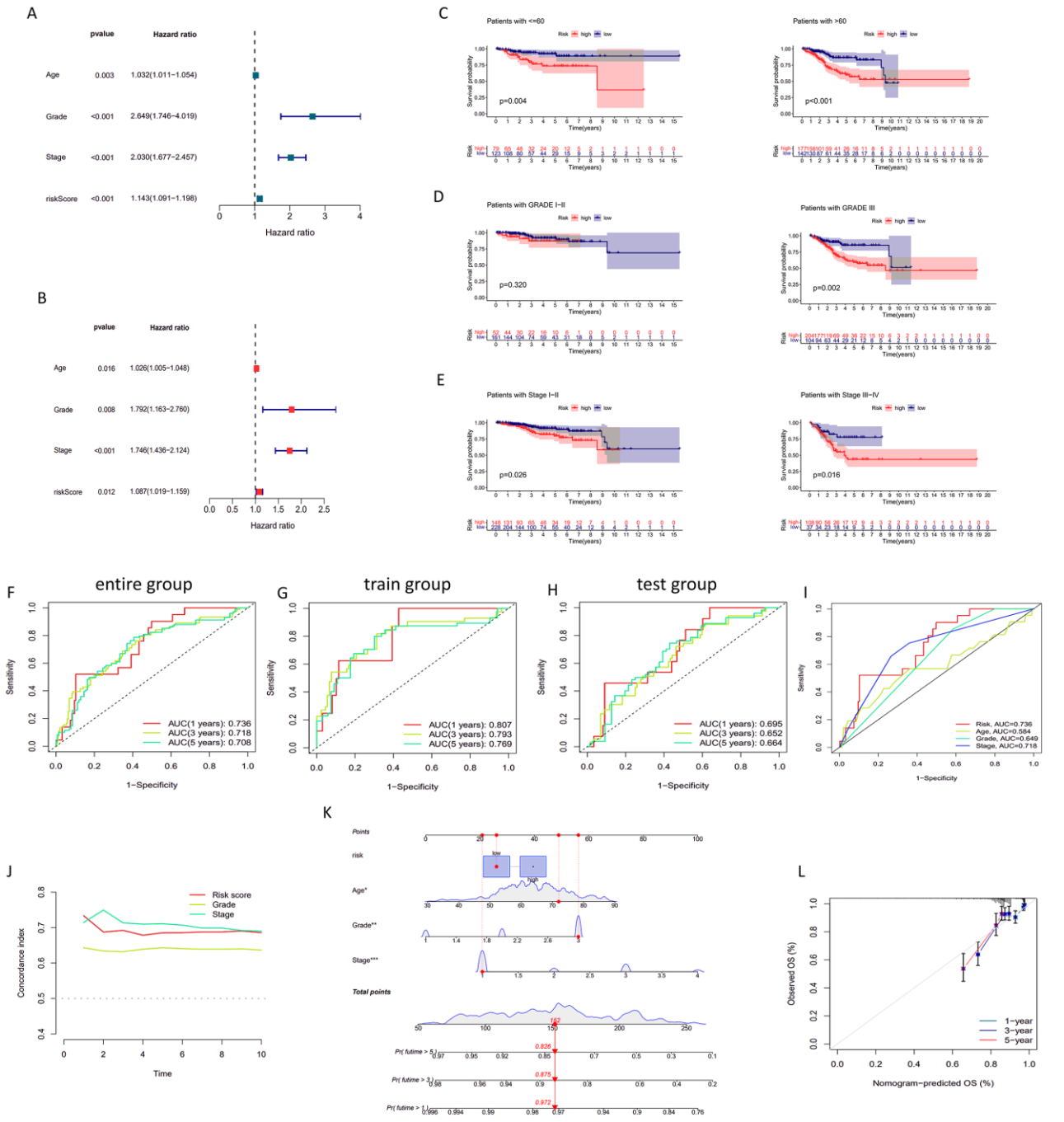

Figure 4. Identification of prognostic independence and accuracy of the gene signature in UCEC. Forest plot of the (A) univariate and (B) multivariate Cox regression analyses in all UCEC cases. (C–E) Kaplan-Meier survival analysis of UCEC patients with high and low risk stratified by age, grade and stage. Time dependent ROC curves for predicting survival in 1, 3, and 5 years in entire (F), training (G) and test (H) groups. (I) ROC curve comparing the prognostic value among risk score, age, grade and stage. (J) Consistence index of risk score, grade and stage in predicting survival. (K) Construction of a nomogram with risk score, age, grade and stage (*$P < 0.05$, **$P < 0.01$, ***$P < 0.001$). Each variable corresponds to a point in the top "Points" bar, indicating its contribution to the overall survival (OS). The total points downward correspond to 1, 3 or 5-year survival possibility. (L) Calibration curve presenting the consensus between nomogram predicted 1, 3, 5-year OS and observed OS.

3.4. GSEA of different risk groups in UCEC

To investigate the functions of differentially expressed genes between high and low-risk groups, we performed GSEA based on gene expression level. The larger the | NES | and the smaller the FDR q value are, the higher the indicated reliability of the enrichment analysis results. In the high-risk group, KEGG enrichment analysis showed highly expressed genes were mainly enriched in the extracellular matrix (ECM) receptor interaction (NES = 2.014, FDR = 0.127), axon guidance (NES = 1.935, FDR = 0.150) and dilated cardiomyopathy pathway (NES = 1.921, FDR = 0.113) (Figure 5A). In the low-risk group, they were enriched in alpha linolenic acid metabolism (NES = -2.169, FDR = 0.005), fatty acid metabolism (NES = -2.141, FDR = 0.004) and ether lipid metabolism (NES = -2.136, FDR = 0.003) (Figure 5B). Table 2 elucidates the top 2 enriched GO terms in BP, MF and CC of differentially expressed genes between high and low risk groups. Highly expressed genes of the high-risk group were enriched in nerve development and voltage gated sodium channel activity, while those of the low-risk group were mainly enriched in cilium movement (Table 2).

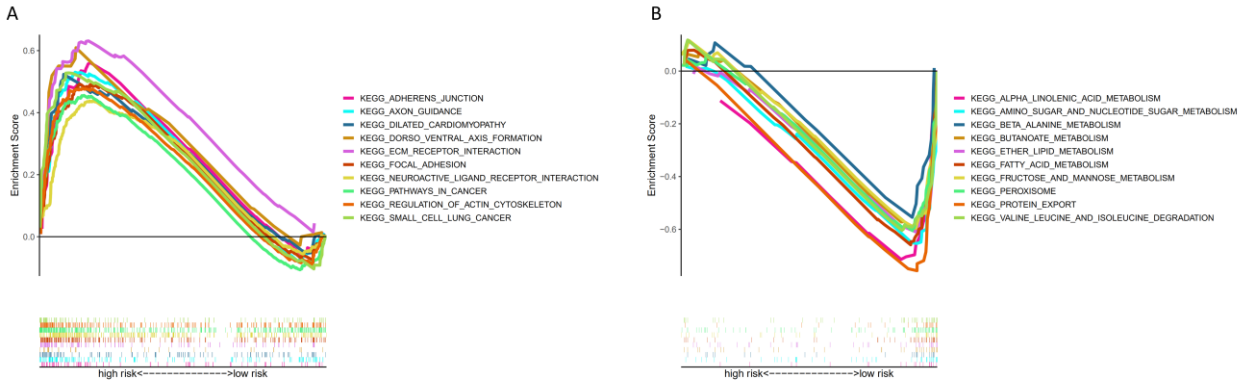

Figure 5. Gene set enrichment analysis (GSEA) of differentially expressed genes between high and low risk groups in Kyoto Encyclopedia of Genes and Genomes (KEGG) pathways. (A–C) Upregulated KEGG pathways in high-risk group with the enrichment score (ES) > 0. (D–F) Upregulated KEGG pathways in low-risk group with the ES < 0.

3.5. Immune infiltration analysis based on the risk model in UCEC

In order to estimate the immune statuses of the two risk groups, we calculated tumor immune microenvironment scores. As shown in Supplementary Figure 2, there was no significant difference between the two groups in stromal score, immune score and ESTIMATE score, indicating the similar tumor purities between different risk groups. We further compared 22 TIICs via CIBERSORT. The results showed the fractions of CD8+ T cells, regulatory T cells (Tregs) and resting dendritic cells in the low-risk group were significantly higher than those of the high-risk group ($P < 0.05$) (Figure 6A). Conversely, the M1 macrophages and activated dendritic cells (aDCs) showed higher infiltration in the high-risk group ($P < 0.05$) (Figure 6A). Immune function analysis showed type I interferon (IFN) response, major histocompatibility complex (MHC) class I, antigen presenting cell (APC) co-inhibition and parainflammation were significantly upregulated in the high-risk group ($P < 0.05$), while type II IFN response and T cell co-stimulation were more active in the low-risk group ($P < 0.05$) (Figure 6B). We

further conducted ssGSEA for immunocytes and immune functions, and the results showed high consistence with those of CIBERSORT. The aDCs were more abundant in high-risk cases ($P < 0.001$), while immature dendritic cells (iDCs), neutrophils and T helper cells were significantly enriched in the low-risk group ($P < 0.05$) (Figure 6C). The immune function analysis results of ssGSEA totally accorded with those of CIBERSORT (Figure 6D). We further investigated the relationship between 22 TIICs and survival. The Kaplan-Meier survival curves showed that UCEC patients with low infiltration of plasma cells and aDCs had more favorable OS ($P < 0.05$) (Figure 6E,I). Highly enriched Tregs, CD8+ T cells and activated neutral killer cells were related with favorable OS ($P < 0.05$) (Figure 6F–H), which might be potential immunotherapy targets.

3.6. Drug sensitivity analysis

To further explore the instructional significance of the risk model for clinical treatment, we analyzed the differences in drug sensitivity between the two risk groups by estimating the IC50. As shown in Figure 7, the IC50 of the drugs, such as cisplatin, cetuximab, bortezomib and navitoclax, were negatively correlated with risk score ($P < 0.001$). Patients with high-risk scores were more sensitive to these drugs, indicating they might be effective anti-UCEC drugs. We further analyzed the small molecular drugs that were sensitive to differentially expressed genes between high and low risk groups via CMap. Table 3 exhibits the top 10 potential sensitive drugs.

Table 3. Screening drugs sensitive to differentially expressed genes between high and low risk groups via Connectivity Map database.

Drug name	MOA	Raw-CS	-log10(FDR)	Norm-CS
Leflunomide	Dihydroorotate dehydrogenase inhibitor, PDGFR inhibitor	-0.5523	15.6536	-1.8867
Pentoxifylline	Phosphodiesterase inhibitor	-0.5303	15.6536	-1.8117
Methiopril	ACE inhibitor	-0.5109	15.6536	-1.7452
Pterostilbene	Cyclooxygenase inhibitor, PPAR receptor agonist	-0.5109	15.6536	-1.7453
Tetramethylsilane	Internal standard for NMR spectroscopy	-0.5057	15.6536	-1.7275
Fostamatinib	Syk inhibitor	-0.5007	15.6536	-1.7105
Ebelactone-b	Lipase inhibitor	-0.5001	15.6536	-1.7085
Tipifarnib-P2	Farnesyltransferase inhibitor	-0.4968	15.6536	-1.6971
Medroxyprogesterone-acetate	Progesterone receptor agonist	-0.4951	15.6536	-1.6914
CO-102862	Sodium channel inhibitor	-0.495	15.6536	-1.6912

MOA: mechanism of action, CS: connectivity score, FDR: false discovery rate, Norm-CS: normalized connectivity score, PDGFR: platelet-derived growth factor receptor, ACE: angiotensin converting enzyme, PPAR: peroxisome proliferator activated receptor, NMR: nuclear magnetic resonance.

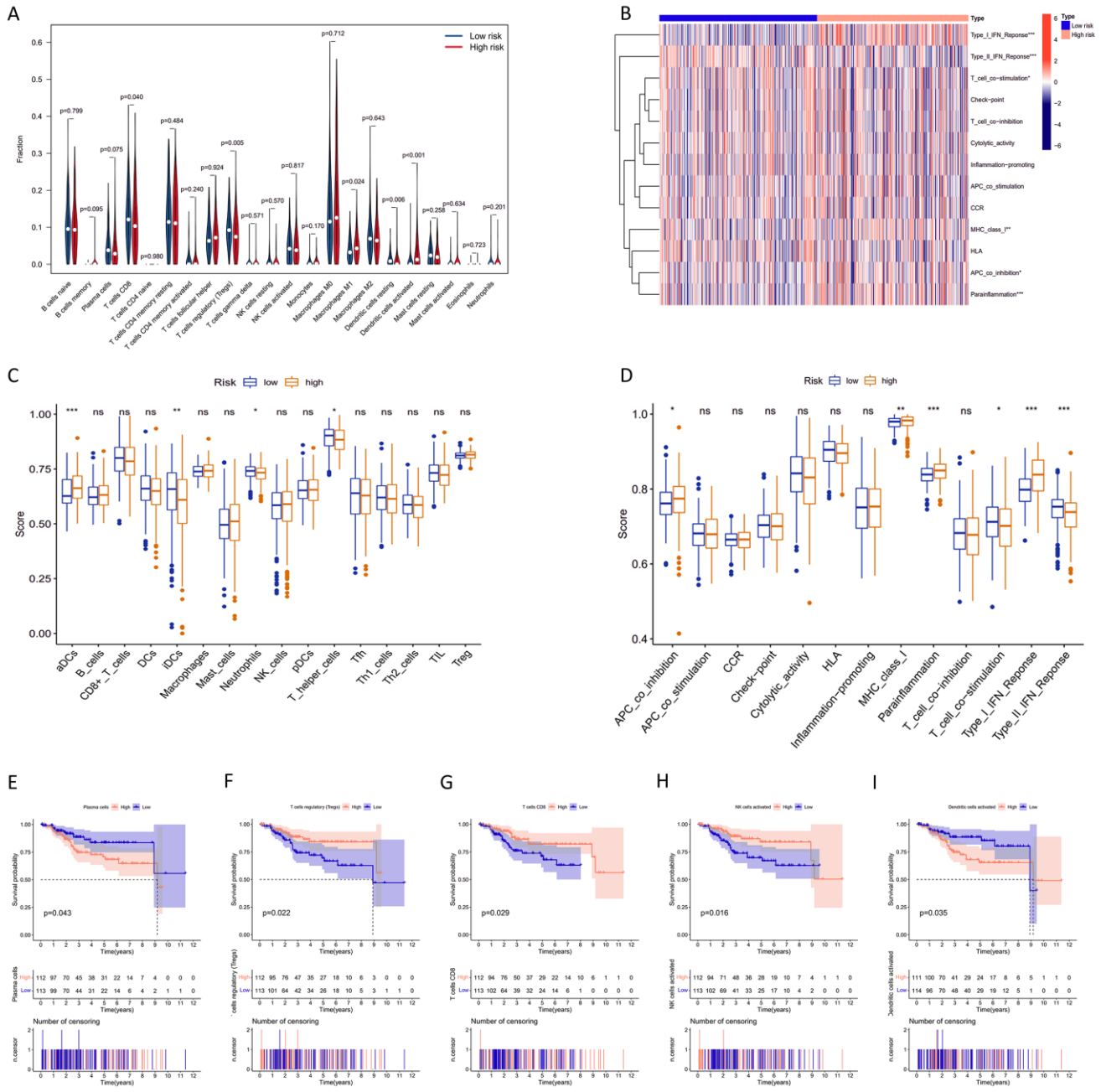

Figure 6. Tumor immune microenvironment analysis and tumor-infiltrating immune cells (TIICs) related survival of two risk groups in UCEC. (A) The violin plots showing the constitution of 22 TIICs in two risk groups via CIBERSORT. (B) The heatmap depicting the immune function of two risk groups. (C–D) The enrichment scores of specific immunocytes (C) and immune functions (D) by single-sample gene set enrichment analysis (ssGSEA). (E-I) Kaplan-Meier survival analysis estimating the prognostic value of 22 TIICs. Only immunocytes with $P < 0.05$ in the log rank test were shown: Those were plasma cells (E), regulatory T cells (F), CD8 T cells (G), activated neutral killer cells (H) and activated dendritic cells (I). *$P < 0.05$, **$P < 0.01$, ***$P < 0.001$, ns: no significance.

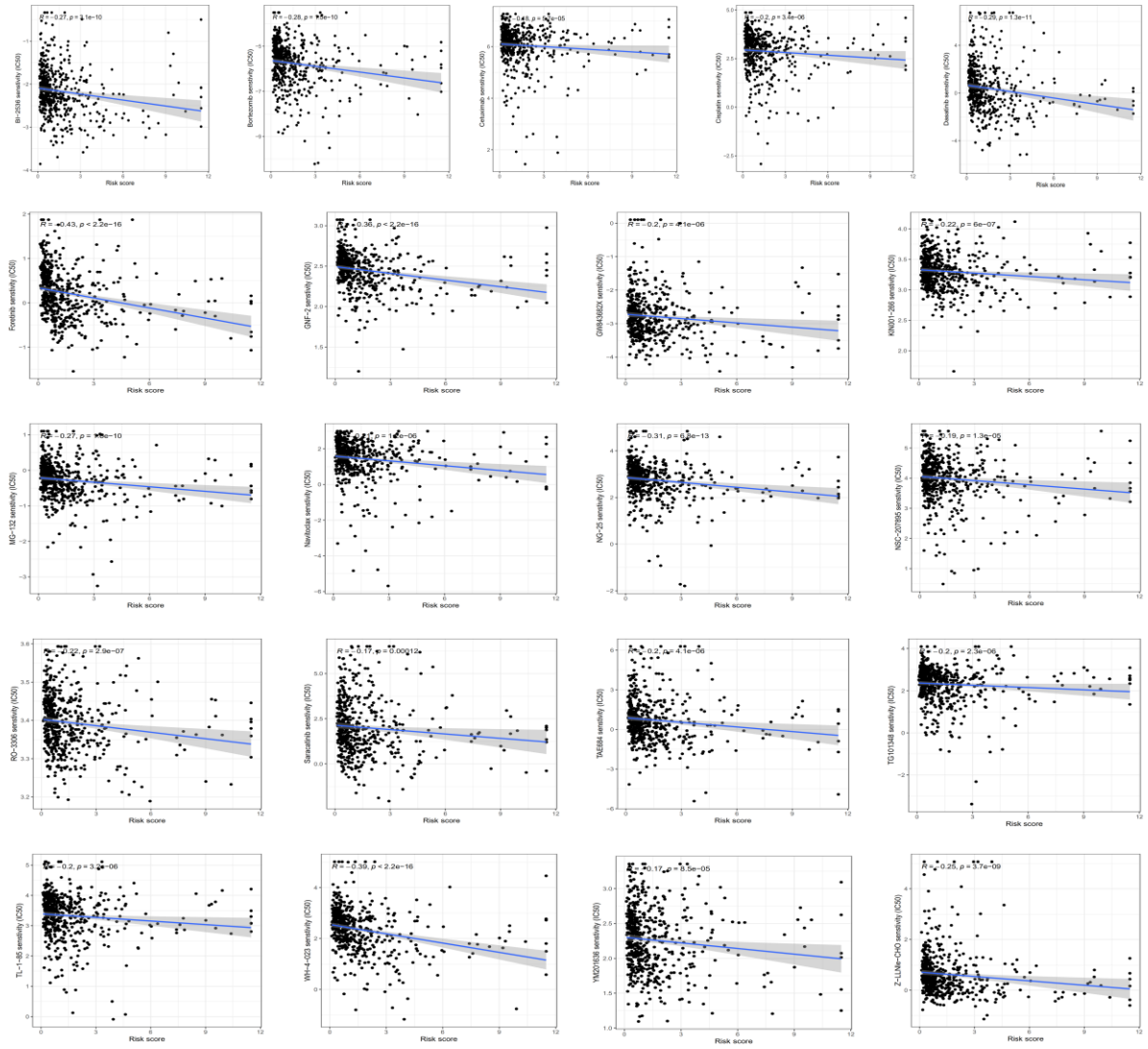

Figure 7. The correlations between drug sensitivity and risk score in UCEC patients by Spearman's correlation analysis. Only drugs with a significantly negative correlation between half-maximal inhibitory concentration (IC50) and risk scores were shown in the scatter plots ($P < 0.001$). The higher the risk score, the lower the IC50, indicating the higher sensitivity to those drugs.

4. Discussion

Due to a growing and ageing population, uterus cancer is predicted to account for 5% of all female cancers in the UK in 2035 with 11,576 cases, a 24.17% increase over 2014 [36]. Given the large number of surviving UCEC patients, survivorship and follow-up to improve their prognosis are crucial [37]. However, there has not been much advancement in UCEC biomarkers or treatment in the last few decades, particularly for advanced and recurrent cases [38]. The treatment of UCEC is multimodal, including accurate surgical staging, proper systemic adjuvant therapies and molecular targeted therapy. Tyrosine kinase inhibitors (TKIs) and immunotherapy have emerged as new treatment

avenues for UCEC [38]. ER plays an essential role in calcium homeostasis, lipid biosynthesis and the synthesis and folding of nearly a third of the protein. ER stress occurs when its ability to fold proteins or dispose of unfolded proteins is compromised, subsequently influencing the cellular function and fate [39]. Numerous studies have proposed that dysregulated UPR secondary to ER stress is involved in tumorigenesis and progression [40,41]. However, ER stress in UCEC has been rarely investigated.

The present study identified DEERGs between UCEC and normal samples and constructed a 4-ERG risk model to predict prognosis and instruct treatment via LASSO regression analysis. Nowadays, gene signatures have been an effective tool to forecast prognosis and assist clinical decision making. ER stress related prognostic risk models have been constructed in various cancers, such as esophageal cancer [42], diffuse glioma [43,44] and hepatocellular cancer [45], but with few reports in UCEC. The risk signature constructed in our present study was validated to possess considerable prognostic accuracy and feasibility. In addition, we constructed a nomogram integrating the risk score and clinical variables, which could effectively predict the 1, 3 and 5-year survival probability of UCEC patients. In addition, we explored the difference of immune infiltration between different risk groups, thereby providing reference for immunotherapy in UCEC. We analyzed the drug sensitivity and screened the sensitive drugs for UCEC patients with different risk scores. Our established signature may serve as a novel biomarker for personalized treatment and ideal follow-up for UCEC patients.

In our study, 4 DEERGs were identified by LASSO Cox regression analysis: namely, ATP2C2, CIRBP, CRELD2 and DRD2. High expression of DRD2 was associated with poor outcome, while the other three were just the opposite (Figure 3D–G). Combined with the results of multivariate Cox regression, DRD2 is a risk factor for UCEC patients' survival. The controversial roles of the 4 genes in various types of cancers have been extensively investigated. For example, in the aspect of etiology of tumors, DRD2 polymorphisms were reported to correlate with reward-motivated behaviors, such as smoking and obesity [46], which may be adverse exposure factors for cancers. Gemignani et al. reported DRD2 polymorphisms could modulate the risk of colorectal cancer [47]. Tan et al. found that higher expression of DRD2 correlated with better survival and could inhibit the tumorigenesis in breast cancer [48], which seems inconsistent with the role in UCEC. Nevertheless, it was reported that DRD2 inhibitor might be a potential therapeutic target in neuroendocrine tumor, prostate cancer and glioblastoma [49,50]. Similarly, as shown in our study, DRD2 may be an adverse factor for the prognosis of UCEC. ATP2C2 is involved in calcium ion homeostasis and was reported to be related to the development and unfavorable OS of breast cancer [51]. CIRBP was reported to negatively correlate with the prognosis of pancreatic ductal adenocarcinoma patients. Inhibiting CIRBP could hinder the tumor progression and enhance treatment sensitivity [52]. CRELD2 was also involved in the progression of breast cancer and could serve as a potential therapeutic target [53]. However, in our multivariate Cox regression, the HRs of ATP2C2, CIRBP and CRELD2 were all below 1, and their high expressions were correlated with better survival, indicating that they may be protective factors for UCEC. Further studies are still needed to investigate their exact roles in UCEC.

Individualized immunotherapy according to molecular classification has been an emerging therapeutic direction for UCEC [54]. The U. S. Food and Drug Administration has approved a series of immunotherapy options, such as pembrolizumab and dostarlimab, to be used in advanced or recurrent UCEC patients with mismatch repair deficient [54,55]. These drugs work by blocking the inhibition of programmed death 1 on T cells. A number of immune-related gene signatures have been established in UCEC with the attempt to shed light on immunotherapy [56–58]. In our study, we analyzed the difference of 22 TIICs between different risk groups. CD8+ T cells and Tregs were more

abundant in the low-risk group, which may be related to better OS of the low-risk group, but previous studies reported controversial results [59,60]. Conversely, aDCs were active in the high-risk group and associated with unfavorable OS. Therefore, a higher TIIC infiltration status may indicate a better prognosis. Strikingly, the TIICs can also predict the response to immunotherapy. UCEC subtypes with high abundance of TIICs may have active anti-tumor response and respond better to immunotherapy [61]. Thus, our risk signature may indirectly predict the response to immunotherapy, but how ER stress influences the anti-tumor immune response in UCEC remains to be elucidated [4].

By R packages and CMap, we investigated potential sensitive anti-UCEC drugs. Notably, among the drugs sensitive to the high-risk group, we mainly screened out several kinds of drugs: TKIs, such as dasatinib, foretinib, and saracatinib; monoclonal antibodies, such as cetuximab; and cell cycle blockers, such as RO-3306 and TAE684 (Figure 7). TKIs are important components in the combination therapy of UCEC. Wang et al. used sunitinib, a multitargeted TKI, prior to radiotherapy and found its radiosensitization activity in endometrial cancer cell lines [62]. A phase 3 clinical trial found that lenvatinib, also a multitargeted TKI, plus pembrolizumab contributed to better prognosis than chemotherapy in advanced UCEC patients [63]. Therefore, our model can relatively accurately predict the sensitive drugs and have implications for treatment. Appropriate treatment should be based on correct clinical stages, pathological grades and molecular classification. More clinical trials and practice are warranted to verify the synergistic effect of combination therapy strategies in UCEC.

However, it must be noted that there are several gaps in our present study. The first is that our data was completely sourced from the TCGA database, so the sample size might be too small to find statistical significance. In addition, the feasibility of the prognostic signature was short of further validation by external databases as well as molecular experiments. What's more, the crosstalk between ER stress and tumor immune microenvironment needs more in-depth molecular mechanism exploration.

5. Conclusions

In conclusion, although further certification is required, our present study proposed a novel ER stress-related risk model, which has been proven not only to have considerable prognostic capacity but also to offer exciting reference for UCEC immunotherapy and drug treatment, thus improving the prognosis of UCEC patients. In the future, we will further investigate its prognostic value and the underlying mechanism by clinical samples and in vitro molecular experiments.

Acknowledgments

Thanks to the TCGA project for providing the original data.

Conflict of interest

The authors declare there is no conflict of interest.

References

1. H. Sung, J. Ferlay, R. L. Siegel, M. Laversanne, I. Soerjomataram, A. Jemal, et al., Global cancer statistics 2020: GLOBOCAN estimates of incidence and mortality worldwide for 36 cancers in 185 countries, *CA: Cancer J. Clin.*, **71** (2021), 209–249. https://doi.org/10.3322/caac.21660
2. K. D. Miller, L. Nogueira, T. Devasia, A. B. Mariotto, K. R. Yabroff, A. Jemal, et al., Cancer treatment and survivorship statistics, 2022, *CA: Cancer J. Clin.*, **72** (2022), 409–436. https://doi.org/10.3322/caac.21731
3. M. Koskas, F. Amant, M. R. Mirza, C. L. Creutzberg, Cancer of the corpus uteri: 2021 update, *Int. J. Gynaecol. Obstet.*, **155** (2021), 45–60. https://doi.org/10.1002/ijgo.13866
4. J. R. Cubillos-Ruiz, S. E. Bettigole, L. H. Glimcher, Tumorigenic and immunosuppressive effects of endoplasmic reticulum stress in cancer, *Cell*, **168** (2017), 692–706. https://doi.org/10.1016/j.cell.2016.12.004
5. X. Chen, J. R. Cubillos-Ruiz, Endoplasmic reticulum stress signals in the tumour and its microenvironment, *Nat. Rev. Cancer*, **21** (2021), 71–88. https://doi.org/10.1038/s41568-020-00312-2
6. Y. Hussain, H. Khan, T. Efferth, W. Alam, Regulation of endoplasmic reticulum stress by hesperetin: Focus on antitumor and cytoprotective effects, *Phytomedicine*, **100** (2022), 153985. https://doi.org/10.1016/j.phymed.2022.153985
7. H. Urra, E. Dufey, T. Avril, E. Chevet, C. Hetz, Endoplasmic reticulum stress and the hallmarks of cancer, *Trends Cancer*, **2** (2016), 252–262. https://doi.org/10.1016/j.trecan.2016.03.007
8. W. M. Shi, Z. X. Chen, L. F. Li, H. Liu, R. Zhang, Q. L. Cheng, et al., Unravel the molecular mechanism of XBP1 in regulating the biology of cancer cells, *J. Cancer*, **10** (2019), 2035–2046. https://doi.org/10.7150/jca.29421
9. J. Khaled, M. Kopsida, H. Lennernas, F. Heindryckx, Drug resistance and endoplasmic reticulum stress in hepatocellular carcinoma, *Cells*, **11** (2022), 632. https://doi.org/10.3390/cells11040632
10. C. Salvagno, J. K. Mandula, P. C. Rodriguez, J. R. Cubillos-Ruiz, Decoding endoplasmic reticulum stress signals in cancer cells and antitumor immunity, *Trends Cancer*, **8** (2022), 930–943. https://doi.org/10.1016/j.trecan.2022.06.006
11. L. Sisinni, M. Pietrafesa, S. Lepore, F. Maddalena, V. Condelli, F. Esposito, et al., Endoplasmic reticulum stress and unfolded protein response in breast cancer: The balance between apoptosis and autophagy and iits role in drug resistance, *Int. J. Mol. Sci.*, **20** (2019), 857. https://doi.org/10.3390/ijms20040857
12. M. Markouli, D. Strepkos, A. G. Papavassiliou, C. Piperi, Targeting of endoplasmic reticulum (ER) stress in gliomas, *Pharmacol. Res.*, **157** (2020), 104823. https://doi.org/10.1016/j.phrs.2020.104823
13. J. C. Wu, S. Qiao, Y. E. Xiang, M. Y. Cui, X. X. Yao, R. X. Lin, et al., Endoplasmic reticulum stress: Multiple regulatory roles in hepatocellular carcinoma, *Biomed. Pharmacother.*, **142** (2021), 112005. https://doi.org/10.1016/j.biopha.2021.112005
14. L. P. Wang, P. C. Fu, Y. Zhao, G. Wang, R. Yu, X. Wang, et al., Dissociation of NSC606985 induces atypical ER-stress and cell death in prostate cancer cells, *Int. J. Oncol.*, **49** (2016), 529–538. https://doi.org/10.3892/ijo.2016.3555

15. G. Cali, L. Insabato, D. Conza, G. Bifulco, L. Parrillo, P. Mirra, et al., GRP78 mediates cell growth and invasiveness in endometrial cancer, *J. Cell. Physiol.*, **229** (2014), 1417–1426. https://doi.org/10.1002/jcp.24578
16. K. Matsuo, M. J. Gray, D. Y. Yang, S. A. Srivastava, P. B. Tripathi, L. A. Sonoda, et al., The endoplasmic reticulum stress marker, glucose-regulated protein-78 (GRP78) in visceral adipocytes predicts endometrial cancer progression and patient survival, *Gynecol. Oncol.*, **128** (2013), 552–559. https://doi.org/10.1016/j.ygyno.2012.11.024
17. D. Hui, C. E. Paiva, F. E. G. Del, C. Steer, J. Naberhuis, W. M. van de, et al., Prognostication in advanced cancer: update and directions for future research, *Support Care Cancer*, **27** (2019), 1973–1984. https://doi.org/10.1007/s00520-019-04727-y
18. D. Hui, J. P. Maxwell, C. E. Paiva, Dealing with prognostic uncertainty: the role of prognostic models and websites for patients with advanced cancer, *Curr. Opin. Support Palliat. Care*, **13** (2019), 360–368. https://doi.org/10.1097/SPC.0000000000000459
19. M. E. Ritchie, B. Phipson, D. Wu, Y. Hu, C. W. Law, W. Shi, et al., limma powers differential expression analyses for RNA-sequencing and microarray studies, *Nucleic Acids Res.*, **43** (2015), e47. https://doi.org/10.1093/nar/gkv007
20. W. Walter, F. Sánchez-Cabo, M. Ricote, GOplot: an R package for visually combining expression data with functional analysis, *Bioinformatics*, **31** (2015), 2912–2914. https://doi.org/10.1093/bioinformatics/btv300
21. K. Ito, D. Murphy, Application of ggplot2 to pharmacometric graphics, *CPT: Pharmacomet. Syst. Pharmacol.*, **2** (2013), e79. https://doi.org/10.1038/psp.2013.56
22. G. Yu, L. G. Wang, Y. Han, Q. Y. He, ClusterProfiler: An R package for comparing biological themes among gene clusters, *OMICS*, 1**6** (2012), 284–287. https://doi.org/10.1089/omi.2011.0118
23. R. Tibshirani, The lasso method for variable selection in the Cox model, *Stat. Med.*, **16** (1997), 385–395. https://doi.org/10.1002/(sici)1097-0258(19970228)16:4<385::aid-sim380>3.0.co;2-3
24. L. Li, Z. P. Liu, Detecting prognostic biomarkers of breast cancer by regularized Cox proportional hazards models, *J. Transl. Med.*, **19** (2021), 514. https://doi.org/10.1186/s12967-021-03180-y
25. P. Blanche, J. F. Dartigues, H. Jacqmin-Gadda, Estimating and comparing time-dependent areas under receiver operating characteristic curves for censored event times with competing risks, *Stat. Med.*, **32** (2013), 5381–5397. https://doi.org/10.1002/sim.5958
26. Y. Yang, H. J. Sun, Y. Zhang, T. F. Zhang, J. L. Gong, Y. B. Wei, et al., Dimensionality reduction by UMAP reinforces sample heterogeneity analysis in bulk transcriptomic data, *Cell Rep.*, **36** (2021), 109442. https://doi.org/10.1016/j.celrep.2021.109442
27. V. P. Balachandran, M. G. Mithat, J. J. Smith, R. P. DeMatteo, Nomograms in oncology: more than meets the eye, *Lancet Oncol.*, **16** (2015), e173–e180. https://doi.org/10.1016/s1470-2045(14)71116-7
28. U. B. Mogensen, H. Ishwaran, A. G. Thomas, Evaluating rrandom forests for survival analysis using prediction error ccurves, *J. Statist. Software*, **50** (2012), 1–23. https://doi.org/10.18637/jss.v050.i11
29. A. Subramanian, P. Tamayo, V. K. Mootha, S. Mukherjee, B. L. Ebert, M. A. Gillette, et al., Gene set enrichment analysis: a knowledge-based approach for interpreting genome-wide expression profiles. *Proc. Natl. Acad. Sci. U. S. A.*, **102** (2005), 15545–15550. https://doi.org/10.1073/pnas.0506580102

30. H. Wickham, The split-apply-combine srategy for data analysis, *J. Statist. Software*, **40** (2011), 1–29. https://doi.org/10.18637/jss.v040.i01
31. K. Yoshihara, M. Shahmoradgoli, E. Martinez, R. Vegesna, H. Kim, W. Torres-Garcia, et al., Inferring tumour purity and stromal and immune cell admixture from expression data, *Nat. Commun.*, **4** (2013), 2612. https://doi.org/10.1038/ncomms3612
32. A. M. Newman, C. B. Steen, C. L. Liu, A. J. Gentles, A. A. Chaudhuri, F. Scherer, et al., Determining cell type abundance and expression from bulk tissues with digital cytometry, *Nat. Biotechnol.*, **37** (2019), 773–782. https://doi.org/10.1038/s41587-019-0114-2
33. S.Hänzelmann, R. Castelo, J. Guinney, GSVA: gene set variation analysis for microarray and RNA-seq data, *BMC Bioinf.*, **14** (2013). https://doi.org/10.1186/1471-2105-14-7
34. P. Geeleher, N. Cox, R. S. Huang, pRRophetic: an R package for prediction of clinical chemotherapeutic response from tumor gene expression levels, *PLoS One*, **9** (2014), e107468. https://doi.org/10.1371/journal.pone.0107468
35. J. Lamb, E. D. Crawford, D. Peck, J. W. Model, I. C. Bla, M. J. Wrobel, et al., The connectivity map: using gene-expression signatures to connect small molecules, genes, and disease, *Science*, **313** (2006), 1929–1935. https://doi.org/10.1126/science.1132939
36. C. R. Smittenaar, K. A. Petersen, K. Stewart, N. Moitt, Cancer incidence and mortality projections in the UK until 2035, *Br. J. Cancer*, **115** (2016), 1147–1155. https://doi.org/10.1038/bjc.2016.304
37. J. Y. Park, J. Y. Lee, Y. Y. Lee, S. H. Shim, D. H. Suh, J. W. Kim, Major clinical research advances in gynecologic cancer in 2021, *J. Gynecol. Oncol.*, **33** (2022), e43. https://doi.org/10.3802/jgo.2022.33.e43
38. J. S. Ferriss, B. K. Erickson, I. M. Shih, A. N. Fader, Uterine serous carcinoma: key advances and novel treatment approaches, *Int. J. Gynecol. Cancer*, **31** (2021), 1165–1174. https://doi.org/10.1136/ijgc-2021-002753
39. S. A. Oakes, Endoplasmic reticulum stress signaling in cancer cells, *Am. J. Pathol.*, **190** (2020), 934–946. https://doi.org/10.1016/j.ajpath.2020.01.010
40. S. K. Hsu, C. C. Chiu, H. U. Dahms, C. K. Chou, C. M. Cheng, W. T. Chang, et al., Unfolded Protein Response (UPR) in survival, dormancy, immunosuppression, metastasis, and treatments of cancer cells, *Int. J. Mol. Sci.*, **20** (2019), 2518. https://doi.org/10.3390/ijms20102518
41. D. Liang, M. Khoonkari, T. Avril, E. Chevet, F. A. E. Kruyt, The unfolded protein response as regulator of cancer stemness and differentiation: Mechanisms and implications for cancer therapy, *Biochem. Pharmacol.*, **192** (2021), 114737. https://doi.org/10.1016/j.bcp.2021.114737
42. X. Xu, Y. Q. Tang, J. S. Zhu, J. H. Luo, Endoplasmic reticulum stress-related four-biomarker risk classifier for survival evaluation in esophageal cancer, *J. Oncol.*, **2022** (2022), 5860671. https://doi.org/10.1155/2022/5860671
43. R. Y. Huang, G. Z. Li, K. Y. Wang, Z. L. Wang, F. Zeng, H. M. Hu, et al., Comprehensive analysis of the clinical and biological significances of endoplasmic reticulum stress in diffuse gliomas, *Front. Cell Dev. Biol.*, **9** (2021), 619396. https://doi.org/10.3389/fcell.2021.619396
44. Q. Zhang, G. F. Guan, P. Cheng, W. Cheng, L. H. Yang, A. H. Wu, Characterization of an endoplasmic reticulum stress-related signature to evaluate immune features and predict prognosis in glioma, *J. Cell. Mol. Med.*, **25** (2021), 3870–3884. https://doi.org/10.1111/jcmm.16321
45. P. Liu, J. H. Wei, F. Y. Mao, Z. C. Xin, H. Duan, Y. Du, et al., Establishment of a prognostic model for hepatocellular carcinoma based on endoplasmic reticulum stress-related gene analysis, *Front. Oncol.*, **11** (2021), 641487. https://doi.org/10.3389/fonc.2021.641487

46. L. M. Morton, S. S. Wang, A. W. Bergen, N. Chatterjee, P. Kvale, R. Welch, et al., DRD2 genetic variation in relation to smoking and obesity in the Prostate, Lung, Colorectal, and Ovarian Cancer Screening Trial, *Pharmacogenet. Genom.*, **16** (2006), 901–910. https://doi.org/10.1097/01.fpc.0000230417.20468.d0
47. F. Gemignani, S. Landi, V. Moreno, L. Gioia-Patricola, A. Chabrier, E. Guino, et al., Polymorphisms of the dopamine receptor gene DRD2 and colorectal cancer risk, *Cancer Epidemiol Biomarkers Prev.*, **14** (2005), 1633–1638. https://doi.org/10.1158/1055-9965.EPI-05-0057
48. Y. Q. Tan, R. Sun, L. Liu, D. J. Yang, Q. Xiang, L. Li, et al., Tumor suppressor DRD2 facilitates M1 macrophages and restricts NF-kappaB signaling to trigger pyroptosis in breast cancer, *Theranostics*, **11** (2021), 5214–5231. https://doi.org/10.7150/thno.58322
49. M. J. Mosquera, S. Kim, R. Bareja, Z. Fang, S. Y. Cai, H. Pan, et al., Extracellular matrix in synthetic hydrogel-based prostate cancer organoids regulate therapeutic response to EZH2 and DRD2 inhibitors, *Adv. Mater.*, **34** (2022), e2100096. https://doi.org/10.1002/adma.202100096
50. L. He, K. Bhat, A. Ioannidis, L. Zhang, N. T. Nguyen, J. E. Allen, et al., Effects of the DRD2/3 antagonist ONC201 and radiation in glioblastoma, *Radiother. Oncol.*, **161** (2021), 140–147. https://doi.org/10.1016/j.radonc.2021.05.027
51. J. Z. Liu, Y. X. Wei, Y. S. Wu, J. Li, J. Z. Sun, G. S. Ren, et al., ATP2C2 has potential to define tumor microenvironment in breast cancer, *Front. Immunol.*, **12** (2021), 657950. https://doi.org/10.3389/fimmu.2021.657950
52. X. Chen, H. Y. Xie, X. Wang, Z. N. Zheng, S. Q. Jin, CIRBP knockdown attenuates tumourigenesis and improves the chemosensitivity of pancreatic cancer via the downregulation of DYRK1B, *Front. Cell Dev. Biol.*, **9** (2021), 667551. https://doi.org/10.3389/fcell.2021.667551
53. S. T. Boyle, V. Poltavets, J. Kular, N. T. Pyne, J. J. Sandow, A. C. Lewis, et al., ROCK-mediated selective activation of PERK signalling causes fibroblast reprogramming and tumour progression through a CRELD2-dependent mechanism, *Nat. Cell. Biol.*, **22** (2020), 882–895. https://doi.org/10.1038/s41556-020-0523-y
54. J. J. A. Marin, M. S. Garcia, G. X. Matias, J. M. Piulats, Facts and hopes in immunotherapy of endometrial cancer, *Clin. Cancer Res.*, **28** (2022), 4849–4860. https://doi.org/10.1158/1078-0432.CCR-21-1564
55. R. Voelker, Immunotherapy approved for endometrial cancer, *JAMA*, **325** (2021), 2143. https://doi.org/10.1001/jama.2021.8319
56. J. H. Liu, Y. C. Wang, J. Mei, S. P. Nie, Y. Zhang, Identification of a novel immune landscape signature for predicting prognosis and response of endometrial carcinoma to immunotherapy and chemotherapy, *Front. Cell Dev. Biol.*, **9** (2021), 671736. https://doi.org/10.3389/fcell.2021.671736
57. G. W. Wang, D. D. Wang, M. G. Sun, X. F. Liu, Q. Yang, Identification of prognostic and immune-related gene signatures in the tumor microenvironment of endometrial cancer, *Int. Immunopharmacol.*, **88** (2020), 106931. https://doi.org/10.1016/j.intimp.2020.106931
58. Y. Meng, Y. B. Yang, Y. Zhang, X. H. Yang, X. M. Li, C. Hu, The role of an immune signature for prognosis and immunotherapy response in endometrial cancer, *Am. J. Transl. Res.*, **13** (2021), 532–548.

59. J. Hu, J. Sun, MUC16 mutations improve patients' prognosis by enhancing the infiltration and antitumor immunity of cytotoxic T lymphocytes in the endometrial cancer microenvironment, *Oncoimmunology*, **7** (2018), e1487914. https://doi.org/10.1080/2162402X.2018.1487914
60. T. Kolben, M. Mannewitz, C. Perleberg, K. Schnell, D. Anz, L. Hahn, et al., Presence of regulatory T-cells in endometrial cancer predicts poorer overall survival and promotes progression of tumor cells, *Cell Oncol. (Dordr)*, 2022. https://doi.org/10.1007/s13402-022-00708-2
61. W. Y. Cao, X. Y. Ma, J. V. Fischer, C. G. Sun, B. H. Kong, Q. Zhang, Immunotherapy in endometrial cancer: rationale, practice and perspectives, *Biomark. Res.*, **9** (2021), 49. https://doi.org/10.1186/s40364-021-00301-z
62. E. Wang, A. Sorolla, Sensitizing endometrial cancer to ionizing radiation by multi-tyrosine kinase inhibition, *J. Gynecol. Oncol.*, **31** (2020), e29. https://doi.org/10.3802/jgo.2020.31.e29
63. V. Makker, N. Colombo, H. A. Casado, A. D. Santin, E. Colomba, D. S. Miller, et al., Lenvatinib plus pembrolizumab for advanced endometrial cancer, *N. Engl. J. Med.*, **386** (2022), 437–448. https://doi.org/10.1056/NEJMoa2108330

AIMS Press